

Effect of Sn⁴⁺ content on properties of indium tin oxide nanopowders

XU Bao-qiang(徐宝强)^{1,2,3}, FENG Rui-kang(冯瑞康)⁴, YANG Bin(杨斌)^{1,2,3}, DENG Yong(邓勇)^{1,2,3}

1. National Engineering Laboratory for Vacuum Metallurgy, Kunming 650093, China;
2. Faculty of Metallurgical and Energy Engineering, Kunming University of Science and Technology, Kunming 650093, China;
3. Key Laboratory for Non-ferrous Vacuum Metallurgy of Yunnan Province, Kunming 650093, China;
4. Henan Yuguang Gold and Lead Group Co., Ltd., Henan 454650, China

Received 6 July 2009; accepted 18 January 2010

Abstract: Indium tin oxide (ITO) nanopowders were prepared by a modified chemical co-precipitation process. The influence of different SnO₂ contents on the decomposition behavior of ITO precursors, and on the phase and morphology of ITO precursors and ITO nanopowders were studied by X-ray diffractometry, transmission electron microscopy and differential thermal and thermogravimetry analysis methods. The TG-DSC curves show that the decomposition process of precursor precipitation is completed when the temperature is close to 600 °C and the end temperature of decomposition is somewhat lower when the doping amount of SnO₂ is increased. The XRD patterns indicate that the solubility limit of Sn⁴⁺ relates directly to the calcining temperature. When being calcined at 700 °C, a single phase ITO powder with 15% SnO₂ (mass fraction) can be obtained. But, when the calcining temperature is higher than 800 °C, the phase of SnO₂ will appear in ITO nanopowders which contain more than 10% SnO₂. The particle size of the ITO nanopowders is 15–25 nm. The ITO nanoparticles without Sn have a spherical shape, but their morphology moves towards an irregular shape when being doped with Sn⁴⁺.

Key words: indium tin oxide (ITO); chemical precipitation; nano-particle; SnO₂

1 Introduction

Transparent conducting oxides (TCOs) with high transparency in the visible region and high conductivity have attracted much attention due to their technological applications[1–2]. Tin-doped indium oxide films (or indium tin oxide films), as a kind of TCO materials, are widely used in a variety of opto-applications such as transparent electrodes in liquid crystal display (LCD), plasma display panels (PDP), organic light emitting diodes (OLEDs), transparent conducting thin films, coating materials in CRTs, solar cells, solid-state image sensors and energy-efficient windows[3–7], due to the wide bandgap of indium oxide (direct gap of 3.55–3.75 eV), good transparency (better than 90% at 550 nm) and low resistivity (10⁻⁵–10⁻⁴ Ω·cm)[8–14].

When SnO₂ is doped in In₂O₃, the electrical

conductivity will increase. The reason is that Sn⁴⁺ doping causes n-type doping of the lattice by providing an electron to the conduction band. But, Sn doping is limited because the solubility limit of Sn⁴⁺ in In₂O₃ is about 6%–8% (mole fraction)[15] with a chemical co-precipitation process. In this work, influence of different SnO₂ contents on ITO nanopowders was investigated using a modified chemical co-precipitation process.

2 Experimental

2.1 Raw materials

The composition of metal indium as the In³⁺ source is listed in Table 1. Tin tetrachloride pentahydrate (A.R.) was used as the Sn⁴⁺ source. 25% ammonia water (A.R.) and ammonia sulfate (A.R.) were used to adjust the pH in the precipitation process and absolute ethanol (A.R.)

Foundation item: Project(U0837604) supported by the Natural Science Foundation of Yunnan Province, China; Project (07C40291) supported by Research Fund of Yunnan Education Department, China; Project (2007003) supported by Research Fund of Kunming University of Science and Technology, China

Corresponding author: YANG Bin; Tel: +86-871-5114017; E-mail: kgyb2005@126.com

DOI: 10.1016/S1003-6326(09)60192-8

Table 1 Composition of metal indium (mass fraction, %)

In	Pb	Zn	Cd	As	Al	Cu	Fe	Sn	Tl	Others
99.995	0.000 5	0.000 5	0.000 4	0.000 5	0.000 3	0.000 4	0.000 5	0.000 4	0.000 3	0.001 2

was used as the dispersion medium in the washing process.

2.2 Experimental procedure

The metal indium was dissolved in dilute sulfuric acid to form indium sulfate solution with 50 g/L In^{3+} , and $\text{SnCl}_4 \cdot 5\text{H}_2\text{O}$ was dissolved in deionized water to make a solution of 30 g/L Sn^{4+} . Mixed solutions corresponding to compositions of 0%, 5%, 10%, and 15% SnO_2 (mass fraction) in ITO powders were prepared. A mixed solution of $(\text{NH}_4)_2\text{SO}_4$ and $\text{NH}_3 \cdot \text{H}_2\text{O}$ with a pH of 9.0 was prepared as the primary reaction liquid in a three-necked bottle in a water bath. By using two different peristaltic pumps, the mixed solution of In^{3+} and Sn^{4+} and 25% ammonia solution were simultaneously added into a reactor in 40 °C water bath with mechanical stirring at 1 000 r/min. In this injection process, the injection rate for the mixed solution of In^{3+} and Sn^{4+} was held constant at 3.0 mL/min and the injection rate for ammonia was adjusted to maintain the pH at 9.0. After the precipitation process, the reaction solution was heated to 80 °C while continually stirring for 1 h, then aged at room temperature for 12 h. The resultant suspension was filtered and washed with deionized water and absolute ethanol by ultrasonic dispersion to remove the residual impurities, such as ammonia sulfate and ammonia chloride. The final filter cake was dried at 85 °C in a vacuum drying oven for 16 h, and then calcined at different temperatures for 4 h to obtain the ITO powders.

2.3 Characterization of ITO powders

The phase and the crystallographic structure of the samples were characterized from their X-ray diffraction (XRD) patterns, recorded using a Rigaku (Japan) D/max-3B X-ray diffractometer equipped with graphite-monochromatized Cu K_α radiation produced at 40 kV and 30 mA. The transmission electron microscopy (TEM, HITACHI H-800) was used to observe the morphology and particle size of the ITO nanopowders. The TG-DSC curves of the samples were recorded using a STA409 PC/PG TGA-DTA analyzer, from the NETZSCH Company in Germany, at 10 °C/min in atmosphere.

3 Results and discussion

3.1 Influence of different SnO_2 contents on ITO precursors

Fig.1 shows the X-ray diffraction patterns of the

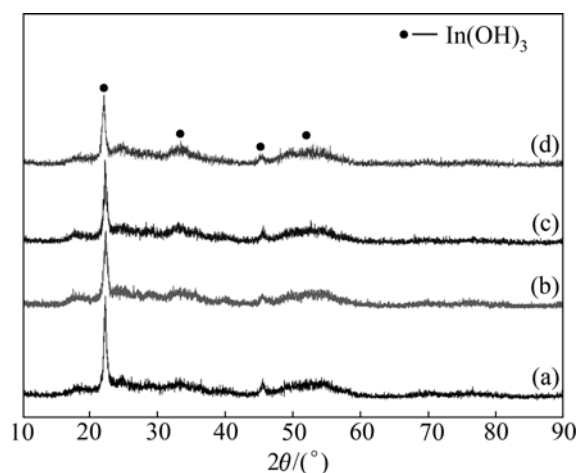


Fig.1 XRD patterns of ITO precursors with different SnO_2 contents: (a) 0; (b) 5%; (c) 10%; (d) 15%

ITO precursors from ITO powders containing 0%, 5%, 10% and 15% SnO_2 . The XRD peaks are consistent with the data of Card 16-0161 in the JCPDS file of $\text{In}(\text{OH})_3$ with a cubic phase[16] and there are no any other crystal peaks, which indicates that the Sn^{4+} has been doped into the precursors. But the amorphous scattering peaks in every pattern indicate that the crystal precursors are not perfect, and depend on the aging time and temperature during the preparation process. When Sn^{4+} is doped, the intensity of the peaks decreases and the peaks are broadened.

Fig.2 shows the TEM images of the ITO precursors corresponding to powders containing 0%, 10% and 15% of SnO_2 . It can be seen from Fig.2 that the SnO_2 content does not significantly affect the grain size of the precipitates, and it can also be seen that these precipitates do not have a perfect crystal shape, which is consistent with the XRD results reported above.

In order to investigate the decomposition behavior and to obtain the calcining temperature of ITO precursors, TG-DSC curves of precipitates corresponding to powders containing 0%, 10% and 15% of SnO_2 were examined and the results are shown in Fig.3. TG curves indicate that the precursors with different SnO_2 contents have similar decomposition behavior. According to the TG-DSC curves, the decomposition process has three main stages. Stage I is a period where adhesive water on the precursors of ITO leaves the surfaces of the ITO precursors below 100 °C. The strongest endothermic peak indicates the process from precursors to ITO powders happening mainly in the range of 100–360 °C in

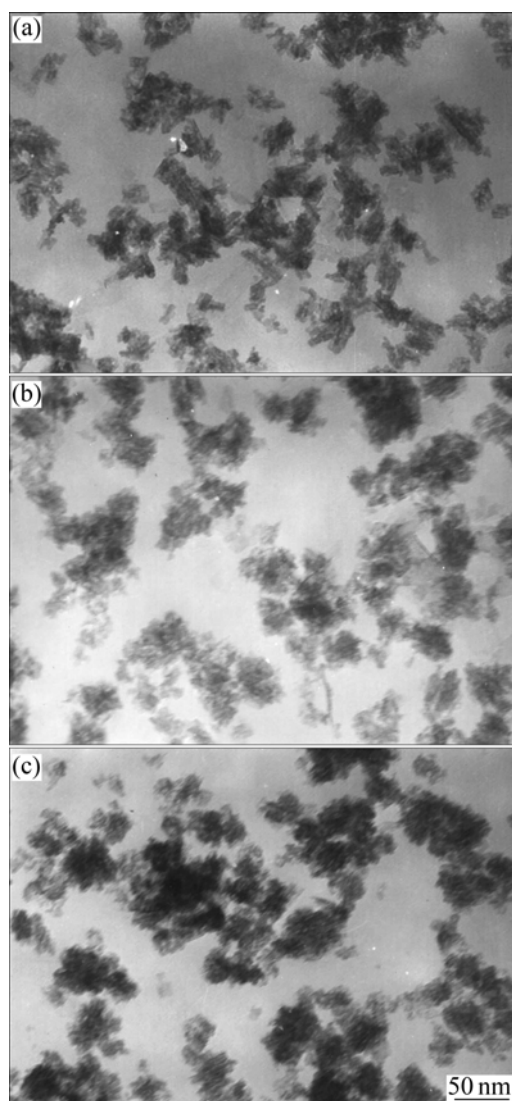


Fig.2 TEM images of ITO precursors: (a) 0% SnO₂; (b) 10% SnO₂; (c) 15% SnO₂

Stage II with the fastest decomposition rate. The rest of the hydration water is removed in Stage III. When the temperature is close to 600 °C, the TG curves tend to flatten to a straight line, which indicates that the decomposition process has finished.

The theoretical mass loss is 16.28% from In(OH)₃ to In₂O₃ and 19.28% from Sn(OH)₄ to SnO₂, which would give mass losses of the precursor powders containing 0, 10% and 15% of SnO₂, of 16.28%, 16.58% and 16.73%, respectively. In Figs.3(a), (b), and (c), the total mass losses of Stage II and Stage III are 16.98%, 17.36 and 17.33%, respectively. These measured mass losses are more than those calculated results from the adhesive water on the surfaces of the ITO precursors. Additionally, Fig.3 suggests that the decomposition temperature will be lower by increasing the doping amount of SnO₂.

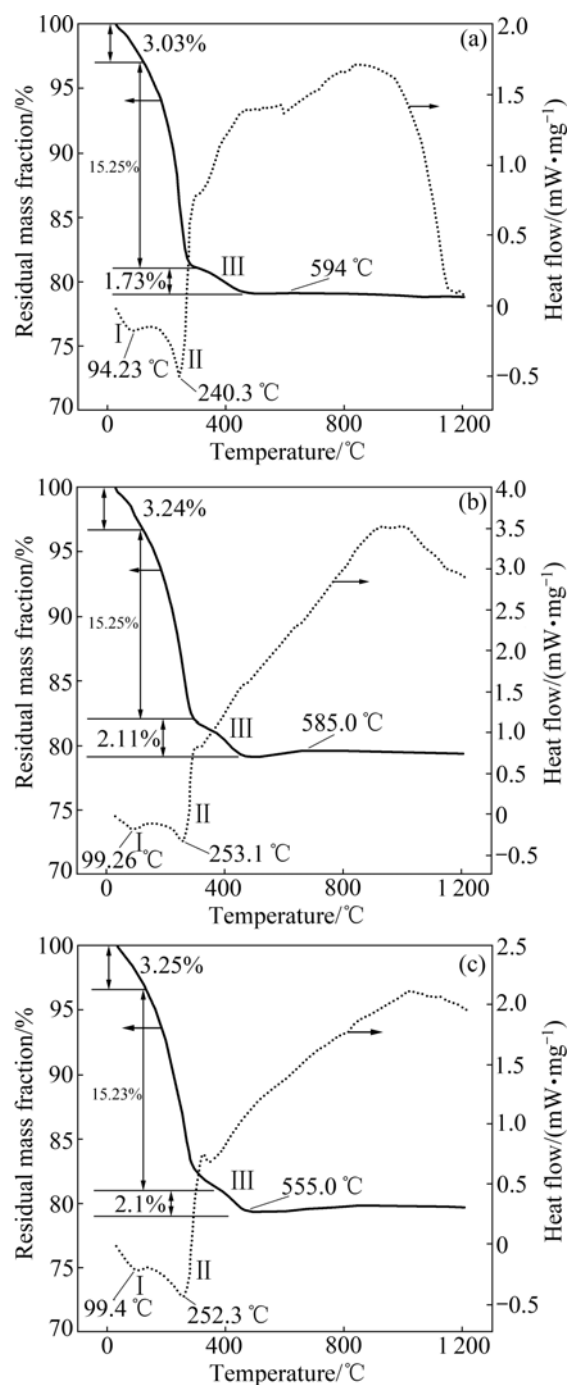


Fig.3 TG-DSC curves of ITO precursors with different SnO₂ contents: (a) 0; (b) 10%; (c) 15%

3.2 XRD analysis of ITO powders doped with different amounts of SnO₂

Figs.4(a) and (b) show the XRD patterns of ITO powders, containing 0, 5%, 10% and 15% SnO₂ sintered for 4 h at 700 °C and 900 °C, respectively. In Fig.4(a), all XRD peaks well match with the data of the Card 6-0416 in the JCPDS file of In₂O₃ with cubic phase[17], which indicates that all SnO₂ is soluble in In₂O₃ and forms a single phase of ITO. The sharp diffraction peaks present the powder of ITO with perfect crystalline. When

sintering at 900 °C in Fig.4(b), the phase SnO₂[15] is seen in the composition of 10% and 15% SnO₂ and it is also observed when being calcined above 800 °C according to the X-ray diffraction patterns of the ITO powders with 10% SnO₂ calcined at different temperatures for 4 h, as shown in Fig.5. This indicates that the higher the calcining

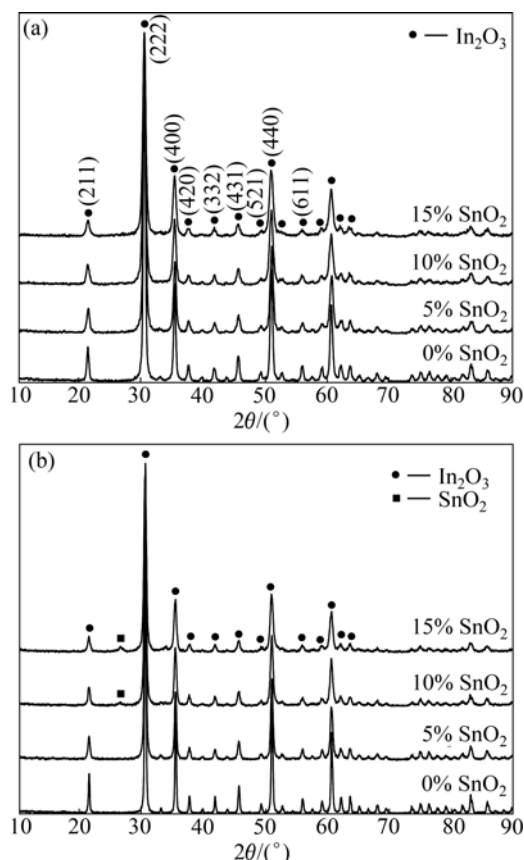


Fig.4 X-ray diffraction patterns of ITO powders with different SnO₂ contents calcined for 4 h at different temperatures: (a) 700 °C; (b) 900 °C

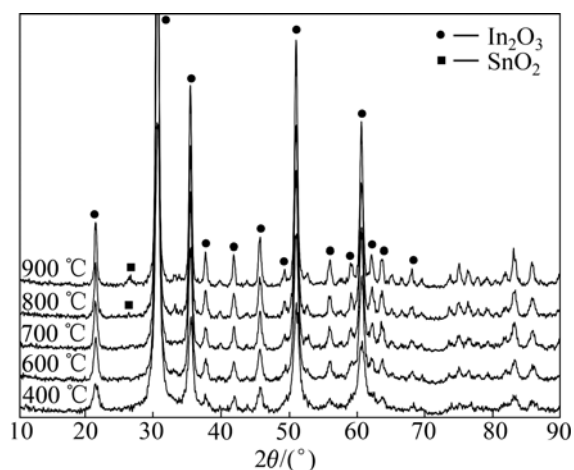


Fig.5 X-ray diffraction patterns of ITO powders with 10% SnO₂ calcined at different temperatures for 4 h

temperature, the lower the solid solubility of SnO₂ in In₂O₃. This result is similar to that of KIM's group but the tin compound phase that appeared in XRD patterns is different from that found in their work[15]. PRAMANIK et al[18] reported that when ITO precursors were calcined at 300 °C, only the cubic phase of In₂O₃ existed up to In-to-Sn ratio of 70:30 (mole fraction, %)[18]. As shown in Fig.5, the XRD peaks become sharper at the higher calcining temperature, which implies that the ITO nanopowders are better crystallized at higher calcining temperatures.

In addition, the XRD peaks of ITO powders are broaden remarkably with increasing SnO₂ content, as seen in Fig.4. The crystalline sizes of the (222) face of crystalline ITO particles with different SnO₂ contents calcined at 700 °C for 4 h were calculated using the Derby-Scherrer formula and the results are given in Table 2, which indicates that doping with SnO₂ makes the ITO particles have smaller crystalline sizes.

Table 2 Crystalline sizes of crystal face (222) on ITO particles with different SnO₂ contents calcined at 700 °C for 4 h

w(SnO ₂)/%	0	5	10	15
Crystalline size/nm	23.46	18.42	17.21	16.48

3.3 Morphology of ITO nanoparticles doped with different SnO₂ contents

Fig.6 shows the TEM images of ITO nanoparticles calcined at 700 °C for 4 h with different SnO₂ contents. It can be seen from Fig.6 that the particle size of the ITO powders is somewhat alike between 15 and 25 nm regardless of the SnO₂ content, and the size of the ITO particles seems to be smaller when Sn⁴⁺ is doped. With respect to the morphology of the ITO nanoparticles, a spherical shape is observed in the case of 0% SnO₂. However, the particles having a spherical shape decrease and the morphology tends towards an irregular shape when Sn⁴⁺ is doped, as in the case of 5%, 10% and 15% SnO₂, which may relate to the fact that doping with Sn⁴⁺ can refine the crystalline of In₂O₃.

4 Conclusions

1) The content of SnO₂ doped into the ITO precursors has no significant effect on the phase, morphology and decomposition behavior of the precipitates in our experiments. TG-DSC curves show that the decomposition process is complete when the temperature is close to 600 °C, and the final decomposition temperature is somewhat lower when the doping amount of SnO₂ is increased.

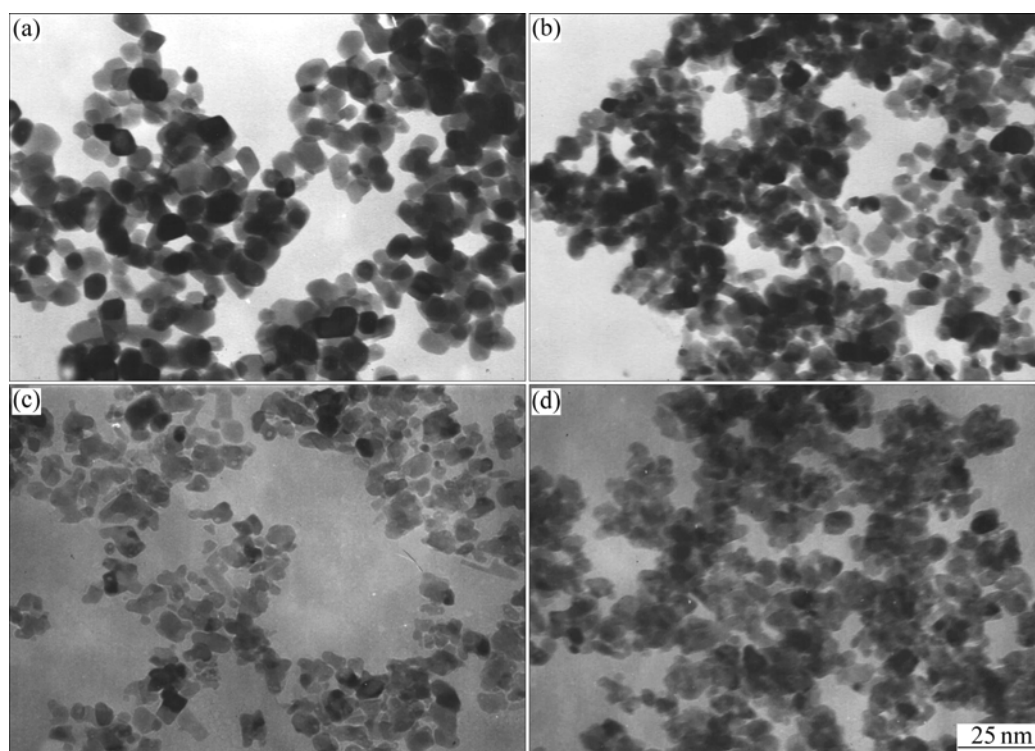


Fig.6 TEM images of ITO nanoparticles calcined at 700 °C for 4 h with different SnO₂ contents: (a) 0%; (b) 5%; (c) 10%; (d) 15%

2) The XRD analysis of the ITO powders indicates that SnO₂ has a certain solubility in ITO powders and that the solubility limit depends on the calcining temperature. When being calcined at 700 °C, a single phase ITO powder with 15% SnO₂ can be obtained. But, when being calcined up to 800 °C, SnO₂ diffraction peaks appear in the XRD patterns of the ITO powders when they contain more than 10% SnO₂.

3) Sn⁴⁺ can reduce the crystalline size of ITO powders according to the broadened XRD peaks, and is confirmed from calculations using the Derby-Scherrer formula. The particle size of ITO nanopowders synthesized by the modified chemical coprecipitation process used in our research is 15–25 nm regardless of the SnO₂ content. ITO nanoparticles with 0% SnO₂ have a spherical shape, but their morphology tends towards an irregular shape when Sn⁴⁺ is doped into the In₂O₃.

Acknowledgments

The authors gratefully acknowledge the help of Professor KAN Jia-de and Professor LIU from Yunnan University, and Professor LI Jian from Kunming University of Science and Technology for their help with the XRD, TEM and TG-DSC analysis.

References

- [1] SONG J E, LEE D K, KIM D K, KIM Y I, KANG Y S. Preparation and characterization of monodispersed indium-tin oxide nanoparticles [J]. *Colloids and Surfaces A: Physicochemical and Engineering Aspects*, 2005, 257/258: 539–542.
- [2] ITO N, SATO Y, SONG P K, KAIJIO A, INOUE K, SHIGESATO Y. Electrical and optical properties of amorphous indium zinc oxide films [J]. *Thin Solid Films*, 2006, 496: 99–103.
- [3] OMANOVIC S, METIKOS H M. A study of the kinetics and mechanisms of electrocrystallization of indium oxide on an in situ prepared metallic indium electrode [J]. *Thin Solid Films*, 2004, 458: 52–62.
- [4] SHIGESATO Y, KOSHI I R, KAWASHIMA T, OHSAKO J. Early stages of ITO deposition on glass or polymer substrates [J]. *Vacuum*, 2000, 59: 614–621.
- [5] KAVEI G, MOHAMMADI G A. The effects of surface roughness and nanostructure on the properties of indium tin oxide (ITO) designated for novel optoelectronic devices fabrication [J]. *Journal of Materials Processing Technology*, 2008, 208: 514–519.
- [6] OUFERFELLI J, OURO D S, BERNEDE J C, CATTIN L, MORSLI M, BERREDJEM Y. Organic light emitting diodes using fluorine doped tin oxide thin films, deposited by chemical spray pyrolysis, as anode [J]. *Materials Chemistry and Physics*, 2008, 112: 198–201.
- [7] LEE W, KWAK C G, MANE R S, MIN S K, CAI G, GANESH T, KOO G, CHANG J, CHO B W, KIM S K, HAN S H. Enhanced photocurrent in RuL₂(NCS)₂/di-(3-aminopropyl)-viologen/SnO₂/ITO system [J]. *Materials Chemistry and Physics*, 2008, 112: 208–212.
- [8] ALFANTAZI A M, MOSKALYK R R. Processing of indium: A review [J]. *Minerals Engineering*, 2003, 16: 687–694.
- [9] PUJILAKSONO B, KLEMENT U, NYBORG L, NYBORG L, JELVESTAM U, HILL S, BURGARD D. X-ray photoelectron spectroscopy studies of indium tin oxide nanocrystalline powder [J]. *Material Characterization*, 2005, 54: 1–7.
- [10] BESBES S, OUADA H B, DAVENAS J, PONSONNET L, JAFFREZIC N, ALCOUFFE P. Effect of surface treatment and

- functionalization on the ITO properties for OLEDs [J]. *Materials Science and Engineering C*, 2006, 26: 505–510.
- [11] GRANQVIST C G, HUTAKER A. Transparent and conducting ITO film: New developments and applications [J]. *Thin Solid Films*, 2002, 411: 1–5.
- [12] KIM G Y, OH J S, CHOI E H, CHO G S, KANG S O, CHO J. Work function change on O-plasma treated indium-tin-oxide [J]. *Materials Science and Engineering B*, 2003, 100: 275–279.
- [13] HAYNES T E, SHIGESATO Y, YASUI I, TAGA N, ODAKA H. Ion beam modification of transparent conducting indium-tin-oxide thin films [J]. *Nuclear Instruments and Methods in Physics Research (Section B): Beam Interactions with Materials and Atoms*, 1997, 121: 221–225.
- [14] SREENIVAS K, MANSINGH A. The growth and structure of RF sputtered indium tin oxide thin films [J]. *Applications of Surface Science*, 1985, 22/23: 670–680.
- [15] KIM S M, SEO K H, LEE J H, KIM J J, LEE H Y, LEE J S. Preparation and sintering of nanocrystalline ITO powders with different SnO₂ content [J]. *Journal of the European Ceramic Society*, 2006, 26: 73–80.
- [16] 16-0161. Joint Committee on Powder Diffraction Standards. Diffraction Data File [S]. 1991.
- [17] 6-0416. Joint Committee on Powder Diffraction Standards. Diffraction Data File [S]. 1991.
- [18] PRAMANIK N C, DAS S, BISWAS P K. The effect of Sn(IV) on transformation of co-precipitated hydrated In(III) and Sn(IV) hydroxides to indium tin oxide (ITO) powder [J]. *Materials Letters*, 2002, 56: 671–679.

(Edited by LI Xiang-qun)